

Influence of Sintering Temperature and Cooling Rate on Microstructure and Mechanical Properties of Pre-alloyed Fe–Cr–Mo Powder Metallurgy Steel

Sandeep Chauhan¹ · Vikas Verma² · U. Prakash² · P. C. Tewari¹ · D. Khanduja¹

Received: 24 December 2015 / Accepted: 13 June 2017 / Published online: 30 June 2017
© The Indian Institute of Metals - IIM 2017

Abstract Influence of carbon content, sintering temperature and cooling rate on microstructure and mechanical properties of a Fe–Cr–Mo alloy has been investigated. Graphite powder with varying wt% (0.4 and 0.8) was mixed with Fe–Cr–Mo prealloyed powder. The green preform compacts of 32 mm diameter were prepared by pressing in a cylindrical die at 650 MPa. The compacts were sintered for 1 h in a flowing gas mixture of 90% N₂ + 10% H₂. Two different sintering temperatures (1120 and 1200 °C) were used. The sintered compacts were cooled at 3.5 °C/min or 6.0 °C/min. It was found that the higher sintering temperature of 1200 °C resulted in improved mechanical properties. Ferrite with pearlite was mostly observed in alloy with 0.4 wt% C while in 0.8 wt% C alloy, a carbide network was also observed. Graphite particles were observed at the prior particle boundaries in some of the alloys. The Fe–Cr–Mo–0.4C alloy processed at 1200 °C with 6.0 °C/min exhibited best strength and ductility. The observed properties were correlated with the microstructure.

Keywords Sintering temperature · Cooling rate · Microstructure · Mechanical properties

1 Introduction

Powder metallurgy (PM) is a cost effective and efficient processing technique to produce near net shape components. PM alloy steels are used in automobile sector to develop mechanical parts for achieving high performance [1–3]. Chawla and Deng [4] sintered Fe–0.85Mo–Ni steels to 96% density through double pressing double sintering process and found that the increased densification resulted in high hardness, tensile and fatigue strength. Campos et al. processed the effect of addition of Mn and graphite in Fe–3Cr–0.5Mo (all compositions in wt%) alloy compacted at 700 MPa and sintered at 1120 °C in a dissociated ammonia atmosphere. He found that the Mn addition from 1 to 2 wt% helped in carbon diffusion at grain boundaries which strengthened the grain bondings resulting high hardness and tensile strength [5]. Narasimhan [6] investigated solid state and liquid state sintering on alloy steels with graphite and/or (Cu, Ni, P, B) additions.

Chromium is widely used in low alloyed wrought steels, since it gives good mechanical properties and has a relatively low cost. In contrast, the usage of chromium in low alloyed PM steels is limited. Wu et al. [7] found that the addition of Cr in Fe–4Ni–1.5Cu–0.5Mo–0.5C alloy increased the tensile strength by 38%, while the impact energy was lowered by 15% and further on quenching, there was an increase in tensile strength by 46% but the impact energy was reduced by 32%. Kremel et al. [8] processed Fe–3Cr–0.5Mo alloy containing 0.2 to 0.5 wt% C at 1120 and 1200 °C and found stronger inter particle bonding at 1200 °C. High temperature sintering of Cr–Mo steels results in more de-oxidation leading to better mechanical properties. Yang Yu studied factors influencing diffusion behavior of carbon as well as Cr and Mo during the sintering of Fe–3Cr–0.5Mo alloy and proposed the

✉ U. Prakash
ujwalfmt@iitr.ac.in; uprakash2@rediffmail.com

¹ Department of Mechanical Engineering, National Institute of Technology, Kurukshetra 136119, India

² Department of Metallurgical and Materials Engineering, Indian Institute of Technology, Roorkee 247667, India

Cooling Curve Transformation diagrams of Fe–Cr–Mo alloy with different carbon wt% (0.3, 0.4 and 0.5) [9]. Carbide formation and oxide layers in Cr–Mo alloy mainly depends on diffusion behavior of carbon as well as high affinity of chromium to oxygen [10–14]. The purpose of this investigation is to study the influence of carbon content, sintering temperature and cooling rate on microstructure and mechanical properties of a Fe–Cr–Mo alloy.

2 Experimental Procedure

The base powder used in this study was a water atomized Astalloy Cr–Mo steel powder. The steel powder was mixed with ultra-fine graphite powder having 2–3 μm size. The powder characteristics of steel powder are shown in Table 1.

The powder sieve analysis is shown in Table 2. The average particle size ($120 \pm 5 \mu\text{m}$) of Fe–Cr–Mo powder was calculated through sieve analysis. The Cr–Mo pre-alloyed powder was mixed with fine graphite powder (0.4 and 0.8 wt%) for 1 h in a ball mill (ball to powder ratio 10:1). The mixed powders were compacted at 650 MPa pressure. Before compaction, the die wall was lubricated with a mixture of acetone and stearic acid. The green compacts were subsequently heated at 5 $^{\circ}\text{C}/\text{min}$ to sintering temperature and sintered for 1 h in a horizontal tubular furnace having MoSi_2 heating elements (Naskar & Company, India) in a flowing gas mixture of nitrogen and hydrogen (90% N_2 + 10% H_2). Two sintering temperature of 1120 and 1200 $^{\circ}\text{C}$ respectively were used in the present work. After sintering, the specimens were cooled to room temperature. Two cooling rates: 3.5 and 6 $^{\circ}\text{C}/\text{min}$ were employed. The density of sintered compacts was calculated by weight and volume measurement. The carbon content of the sintered specimen was determined by a Leco carbon

and sulphur analyzer. The hardness of sintered compacts was determined using 10 kg load in a Vickers Hardness Testing Machine, FIE VM50 India. Tensile samples of gauge diameter 4 mm were prepared as per ASTM E8M standard. Tensile tests were performed using H-25K tensile testing machine. For optical microscopy (OM) under a Leica Model 5000M microscope, the steel samples were mechanically polished to one micron grade alumina powder finish and etched with 2% Nital solution. The volume fraction of phases present as well as porosity in the samples were calculated using the image analyzer software. Polished samples were examined in a scanning electron microscope (SEM), (S4300, Hitachi Ltd., Japan or FESEM, Quanta 200 FEG, the Netherlands) equipped with energy dispersive X-ray spectroscopy (EDS, Oxford Instruments). Rigaku Smartlab X-ray diffractometer (G8, Bruker, Germany) was used for phase identification.

3 Results and Discussion

After compaction, cylindrical compacts with a green density of $\sim 7.2 \text{ g}/\text{cm}^3$ are obtained. The carbon content of sintered compacts has been found to be 0.35–0.68 wt% respectively. It is lower than the amount of admixed graphite indicating that 15–20% of graphite is lost due to decarburization during sintering. There is only a marginal increase in density after sintering indicating the high compressibility of the powder used. Typical porosity in the sintered samples is found to be 6–7%.

Figure 1 shows the microstructure of Fe–Cr–Mo, Fe–Cr–Mo–0.4C and Fe–Cr–Mo–0.8C alloys sintered at 1120 $^{\circ}\text{C}$ and cooled at 3.5 $^{\circ}\text{C}/\text{min}$. Microstructure comprises mainly of ferrite (light), pearlite (grey) and cementite (dark). Fe–Cr–Mo consists of ferrite grains with oxides at prior particle boundaries (Fig. 1a) while Fe–Cr–Mo–0.4C consists of mixture of ferrite and pearlite with some carbide at the boundaries (Fig. 1b). In Fe–Cr–Mo–0.8C, relatively more pearlite and carbide are observed due to higher carbon content of the alloy. Also some graphite is observed at the boundary, which weakens the bond between the grains and lowers the strength at 0.8 wt%C.

Similar microstructures are obtained in other sintered compacts (Figs. 2, 3, 4). Volume fraction measurement of ferrite, pearlite and cementite present in the sintered sample is summarized in Table 3. Increasing sintering temperature lowers the amount of ferrite and increases pearlite volume fraction. This may be related to higher diffusivity of carbon at higher temperature. However the volume fractions of pearlite observed are significantly lower than the equilibrium volume fractions at these compositions (around 50% pearlite in 0.4 wt% and 100% pearlite in 0.8 wt%). Further no free carbide is expected under

Table 1 Powder characteristics of Fe–Cr–Mo pre-alloyed steel as supplied by the manufacturer

Sr. no.	Properties	Cr–Mo pre-alloyed steel
1	Apparent density (g/cm^3)	2.77
2	Flow rate (s/50 g)	29
3	Compressibility (g/cm^3) at 600 MPa	6.99
4	Composition	2.94 wt% Cr and 0.5 wt% Mo (Base Fe)

Table 2 Sieve analysis of Fe–Cr–Mo pre-alloyed steel

Sieve size (μm)	+180	+125	+105	+90	+74	+53
wt%	10.4	50.4	30.8	7.0	4.0	1.0

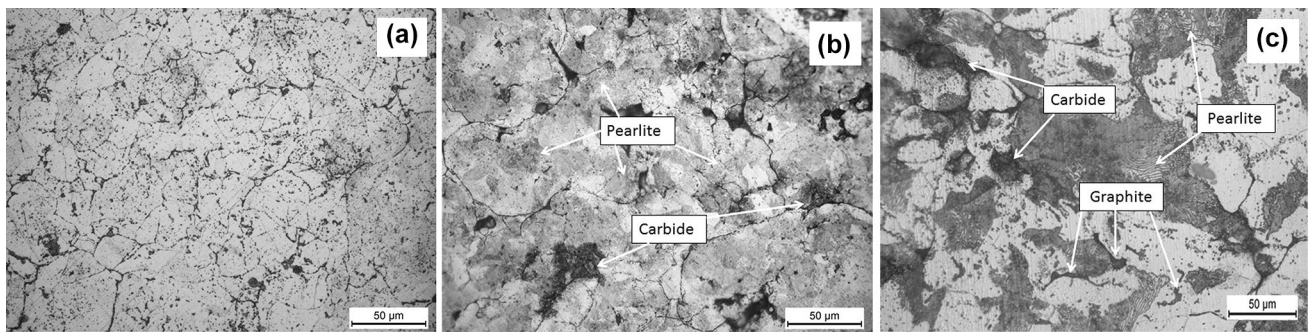


Fig. 1 Microstructure at sintering temperature 1120 °C with 3.5 °C/min cooling rate, **a** Fe–Cr–Mo, **b** Fe–Cr–Mo–0.4C and **c** Fe–Cr–Mo–0.8C

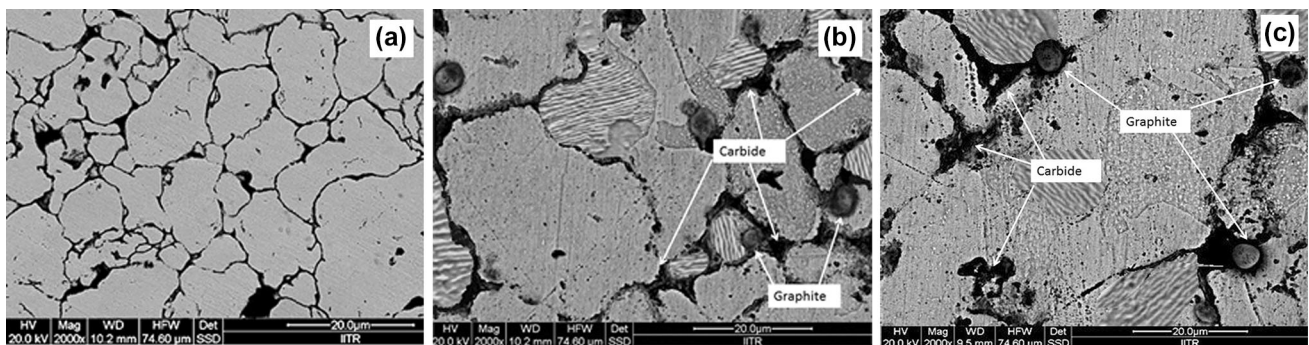


Fig. 2 SEM (BSE) micrograph at sintering temperature 1200 °C with 3.5 °C/min cooling rate, **a** Fe–Cr–Mo, **b** Fe–Cr–Mo–0.4C and **c** Fe–Cr–Mo–0.8C

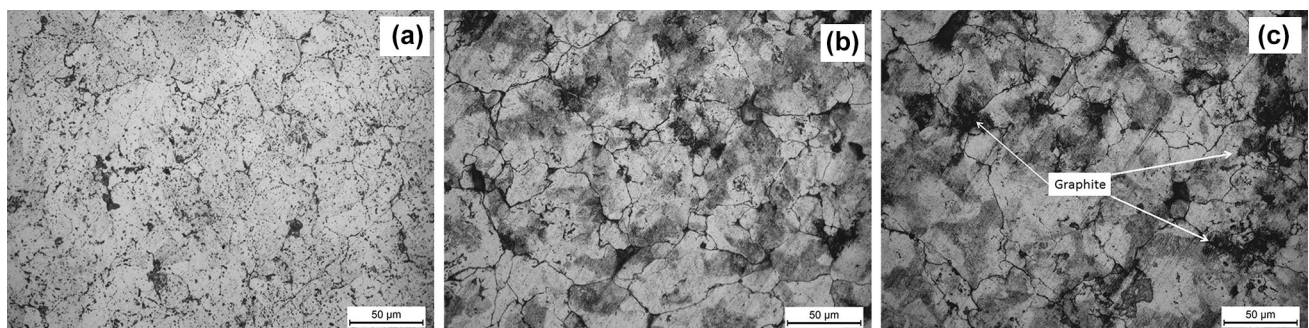


Fig. 3 Microstructure at sintering temperature 1120 °C with 6.0 °C/min cooling rate, **a** Fe–Cr–Mo, **b** Fe–Cr–Mo–0.4C and **c** Fe–Cr–Mo–0.8C

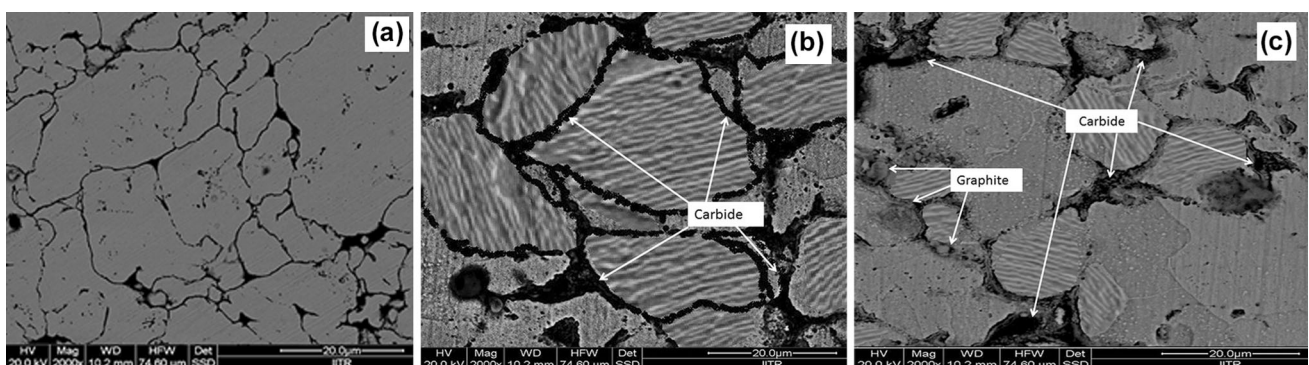


Fig. 4 SEM (BSE) micrograph at sintering temperature 1200 °C with 6.0 °C/min cooling rate, **a** Fe–Cr–Mo, **b** Fe–Cr–Mo–0.4C and **c** Fe–Cr–Mo–0.8C

Table 3 Volume fraction of ferrite, pearlite and carbide formed after sintering

Cooling rate (°C/min)	Sintering temperature (°C)	0.4 wt% Graphite			0.8 wt% Graphite		
		Ferrite	Pearlite	Carbide	Ferrite	Pearlite	Carbide
3.5	1120	40.33	40.94	9.70	25.22	42.78	22.74
	1200	35.45	47.28	8.20	22.89	49.46	18.64
6.0	1120	41.56	44.38	7.76	29.11	44.29	17.15
	1200	32.80	50.14	7.10	25.83	47.15	20.38

equilibrium in alloy containing 0.8 wt%C. Thus the alloys have experienced non-equilibrium processing conditions. Increase in carbon content increases the pearlite/carbide volume fraction. The cooling rate appears to have only a marginal effect on the microstructure.

The region near grain boundaries has been examined with the help of energy dispersive spectroscopy (EDS) analysis. Figure 5a, c, e show the composition within the grains. The elements presented at boundary are shown in Fig. 5b, d, f. Alloys show carbon enrichment at the grain boundaries with increasing carbon content. Mechanical properties of Fe–Cr–Mo alloy are highly influenced by the addition of carbon content, sintering temperature and cooling rates. Higher volume fraction of pearlite and absence/very little presence of graphite at prior particle boundaries in Fe–Cr–Mo alloy with 0.4 wt% C sintered at 1200 °C result in higher hardness, yield strength and ultimate tensile strength (Figs. 6, 7). At 0.8 wt%C, there is undissolved graphite at prior particle boundaries. This decreases the mechanical properties for both the cooling rates (3.5 and 6.0 °C/min). Hardness (230 HV10), yield strength (274 MPa) and ultimate tensile strength (325 MPa) are maximum for Fe–Cr–Mo–0.4C alloy sintered at 1200 °C temperature with cooling rate of 6.0 °C/min (Figs. 6, 7).

It has been reported in literature that sintering at a high temperature (1200 °C) reduces oxide formation and improves mechanical properties [12]. In view of present results, a high sintering temperature may also be beneficial for carbide dissolution and is responsible for higher pearlite/carbide content in alloys sintered at 1200 °C. This in turn also improves the mechanical properties. Campos et al. studied that the Fe–Cr–Mo alloy with graphite wt% of 0.35 compacted at 700 MPa pressure and sintered at 1120 °C and cooled at 9 °C/min exhibit hardness of 230 HV, yield strength 96 MPa and tensile strength of 483 MPa with percentage elongation of 0.85% [5]. The low

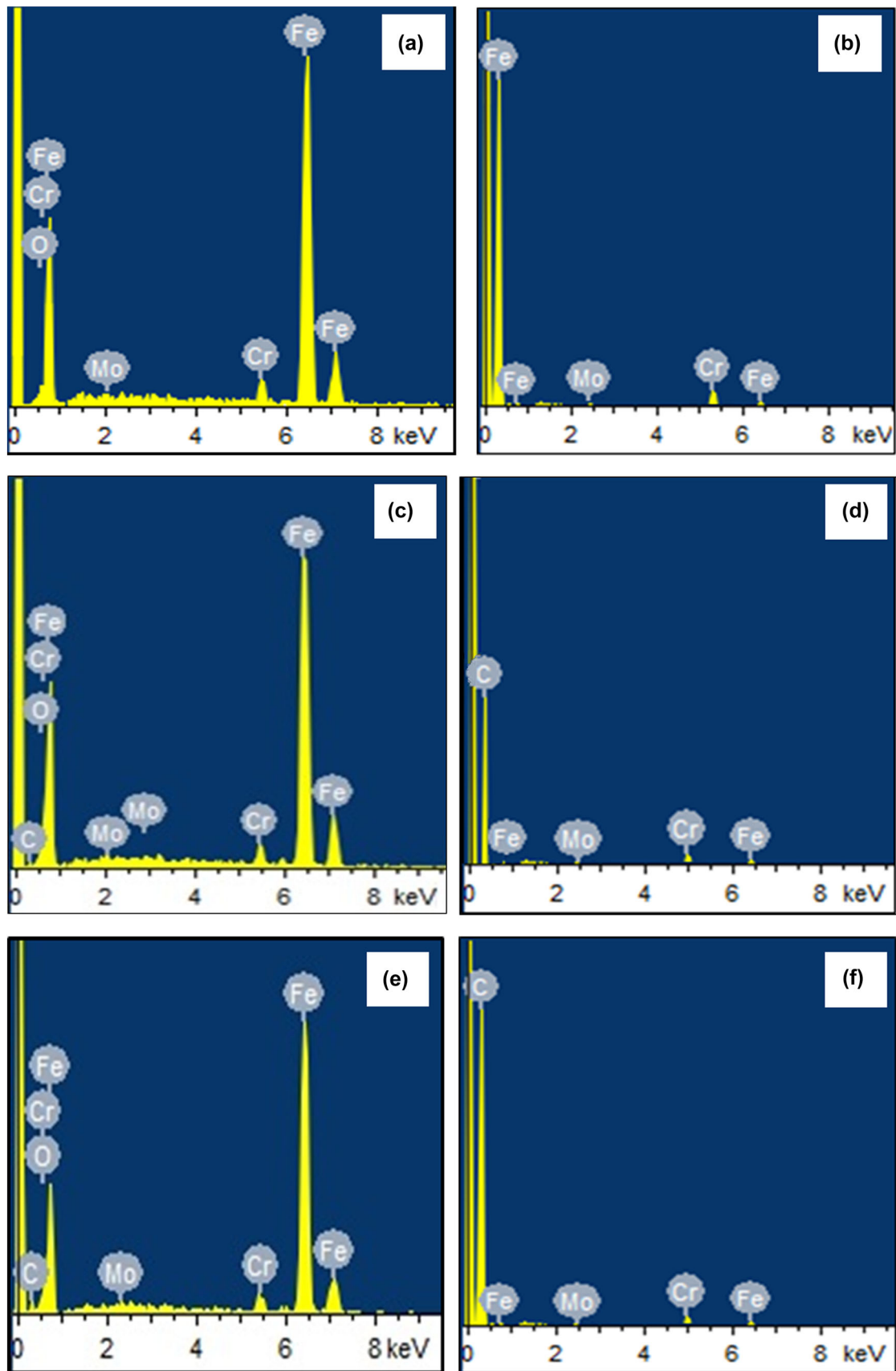
Fig. 5 a, b Typical area and point EDS Spectra from sintered compacts of Fe–Cr–Mo, **c, d** Fe–Cr–Mo–0.4C and **e, f** Fe–Cr–Mo–0.8C sintered at 1200 °C and subsequently cooled at the rate of 6.0 °C/min

value of elongation is due to porosity in the samples. The tensile elongation observed in the present work is limited to 3% also due to porosity present in the samples. Presence of porosity in the sintered samples processed via PM route helps in lubrication as in applications of automobile transmission systems (bearings, gears etc.), where oil penetrates through pores and gives lubricating effect [1–3]. The compositions studied in the present work have potential for similar applications. At high carbon levels, some graphite is left at prior particle boundaries. It is thus recommended that carbon levels in sintered compacts be maintained close to 0.4 wt%.

4 Conclusions

Present study of Fe–Cr–Mo pre-alloyed steel with 0.4 and 0.8 wt% C sintered at 1120 and 1200 °C with 3.5 and 6.0 °C/min led to the following conclusions:

1. The higher sintering temperature may be beneficial for carbide dissolution. Increasing sintering temperature also increases the amount of pearlite/carbide percent. It may also lead to reduced oxide in sintered compacts leading to improved mechanical properties.
2. Presence of graphite at prior particle boundaries at 0.8 wt% C decreases the mechanical properties of sintered compacts. It is thus recommended that carbon levels in sintered compacts be maintained close to 0.4 wt%.
3. The Fe–Cr–Mo pre-alloyed with 0.4 wt% C addition sintering at 1200 °C with 6.0 °C/min cooling rate



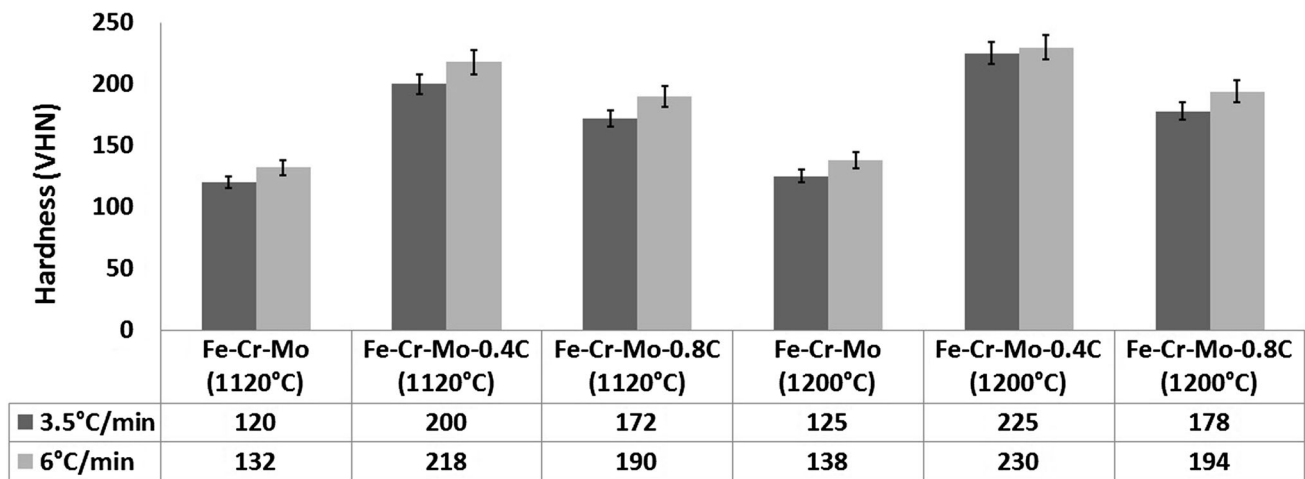


Fig. 6 Hardness value at different cooling rates and sintering temperatures

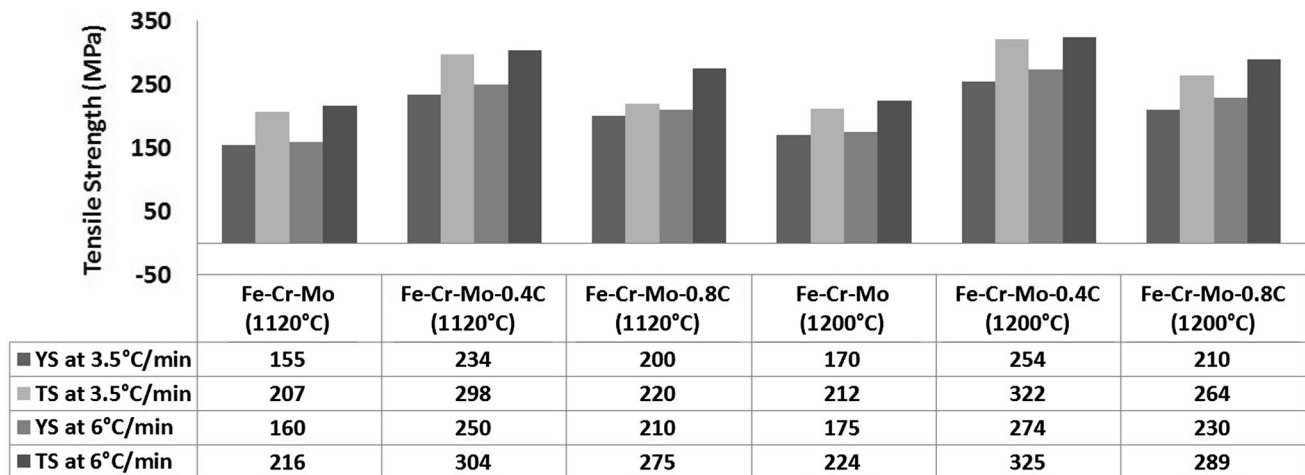


Fig. 7 Tensile strength and yield strength at different sintering temperatures and cooling rates

promotes the higher tensile strength i.e. 325 MPa with higher yield strength of 274 MPa and hardness value 230 at HV10 load.

Acknowledgements We are highly thankful to Dr. B.V. Manoj Kumar, Faculty of M.M.E.D., I.I.T. Roorkee for the facility of high temperature sintering furnace. Hogan India provided Astaloy CrM powder and Oxeco, Hyderabad provided graphite powder free of cost for this work. One of the authors (SC) acknowledges support of MHRD fellowship from Government of India.

References

- German R, *Powder Metallurgy Science*, Metal Powder Industries Federation, Princeton, NJ (1984), p 2.
- Salak A, *Ferrous Powder Metallurgy*, Cambridge International Science Publishing, Cambridge (1997), p 1.
- Hadrboletz A, and Weiss B, *Int Mater Rev* **42** (1997) 1.
- Chawla M, and Deng X, *Mater Sci Eng A* **390** (2005) 98.
- Campos M, Sanchez D, and Torralba J M, *J Mater Process Technol* **143** (2003) 464.
- Narasimhan K S, *Mater Chem Phys* **67** (2001) 56.
- Wu M W, Tsao L C, and Chang S Y, *Mater Sci Eng A* **565** (2013) 196.
- Kremel S, Danninger H, and Yu Y, *Powder Metall Prog* **2** (2002) 211.
- Yu Y, PM2000 in Kyoto, Japan (2000).
- Bergman O, *Powder Metall* **50** (2007) 243.
- Bergman O, Lindqvist B, and Bengtsson S, *Mater Sci Forum* **534** (2007) 545.
- Ortiz P, and Castro F, *Powder Metall* **47** (2004) 291.
- Hrubovlakova M, Dudrova E, Hryha E, Kabatova M, and Harvanova J, *Adv Mater Sci Eng* (2013) 1.
- Hrubovcakova M, Dudrova E, and Harvanova J, *Powder Metall Prog* **11** (2011) 1.